

We are IntechOpen, the world's leading publisher of Open Access books Built by scientists, for scientists

5,500

Open access books available

135,000

International authors and editors

165M

Downloads

Our authors are among the

154

Countries delivered to

TOP 1%

most cited scientists

12.2%

Contributors from top 500 universities



WEB OF SCIENCE™

Selection of our books indexed in the Book Citation Index
in Web of Science™ Core Collection (BKCI)

Interested in publishing with us?
Contact book.department@intechopen.com

Numbers displayed above are based on latest data collected.
For more information visit www.intechopen.com



Dual Source, Dual Energy Computed Tomography in Pulmonary Embolism

Yan'E Zhao¹, Long Jiang Zhang¹, Guang Ming Lu¹,
Kevin P. Gibbs² and U. Joseph Schoepf²

¹Department of Medical Imaging, Jinling Hospital, Clinical School of Medical College,
Nanjing University, Nanjing, Jiangsu Province

²Department of Radiology and Radiological Science
Medical University of South Carolina, Ashley River Tower

¹China

²USA

1. Introduction

More than 650,000 cases of pulmonary embolism (PE) are reported each year, resulting in an estimated 300,000 annual fatalities. This level of occurrence ranks PE as the third leading cause of death in the USA [Laack TA, 2004; Tapson VF, 2008]. Multidetector CT (MDCT) pulmonary angiography has now largely replaced ventilation/perfusion scintigraphy and conventional pulmonary angiography for the evaluation of possible PE [Patel S, 2003]. In 2007, MDCT pulmonary angiography was accepted as the reference standard for diagnosis of acute PE [Remy-Jardin M, 2007]. However, conventional MDCT pulmonary angiography only provides morphological information and its ability to assess subsegmental pulmonary arteries is variable: sensitivities range from 37%–96%. The ability to assess subsegmental pulmonary arteries has increased with advances in MDCT technology.

In the past, various CT techniques have been developed to evaluate the assessment of lung perfusion in patients with suspected PE. (1) Dynamic multi-section electron beam CT [Schoepf UJ, 2000]. This perfusion-based CT technique had a scanning volume of 7.6 cm, required a long patient breathhold, and delivered a high additional radiation dose to the patient. (2) Color-coding the density of lung parenchyma in contrast-enhanced CTA [Wildberger JE, 2001]. This technique is of limited use when lung diseases, such as ground-glass opacities (e.g., in pulmonary edema or pneumonia) were present. (3) A subtraction CTA technique of whole-thorax multi-detector CT scans acquired before and after intravenous contrast within a single breathhold. This technique was limited by a longer breathhold time, misregistration artifacts because of the mismatched unenhanced and contrast-enhanced scans, and additional radiation dose caused by the fact that an additional unenhanced scan had to be performed to assess the iodine distribution in the lung [Wildberger JE, 2005].

Recently, DECT with different dual energy CT hardware (dual source CT and rapid kV switching technique) became available to simultaneously provide the functional and morphological information, overcoming the limitations of the above-mentioned CT

perfusion techniques. Iodine, shows a proportionally larger increase of CT values with decreasing X-ray tube voltage compared to other materials, e.g., to soft tissue, iodinated contrast medium enhanced DECT provides the opportunity to assess pulmonary parenchyma iodine maps (i.e., lung perfusion). Compared with the previously developed CT perfusion techniques, DECT technique eliminates registration problems and allows selective visualization of iodine distribution with high spatial resolution and no additional radiation exposure to the patient compared with the conventional CT pulmonary angiography technique.

This chapter will present the techniques, scanning and contrast medium injection protocols, image postprocessing and image interpretation, clinical applications and radiation dose of dual source, dual energy CT pulmonary angiography.

2. Techniques

Recent generations of MDCTs are able to acquire dual-energy data by applying two X-ray tubes and two corresponding detectors at different kVp and mA settings simultaneously in a dual-source CT (Siemens Healthcare), by ultra-fast kVp switching in a single source CT (GE Healthcare) or by compartmentalization of detected X-ray photons into energy bins by the detectors of a single-source CT operating at constant kVp and mA settings (Philips Healthcare). The dual-source CT scanner is composed of two x-ray tubes and two corresponding detectors. The two acquisition systems are mounted on the rotating gantry with an angular offset of 90°/95° with regard to their kilovoltage and milliamperage settings. For dual-energy CT acquisition, the tube voltages are set at high energy (140 kVp) for tube A and low energy (80 kVp) for tube B. The rapid kilovoltage switching technique from GE Healthcare uses a single x-ray source. A generator electronically switches rapidly the tube energies from low energy (80 kVp) to high energy (140 kVp) and back again to acquire dual-energy images. Each exposure takes about 0.5 msec.

3. Scanning injection protocols

3.1 Scanning protocols

The protocol aims to display both the pulmonary arteries and lung perfusion from a single contrast-enhanced CT scan. Various scanning protocols with dual source dual energy CT scanners have been proposed in the literature [Fink C, 2008], but currently there are few published protocols for CT systems of other vendors [Thieme SF, 2009]. The scan protocols recommended for dual-energy lung perfusion scans by dual-source CT (Siemens) are presented in Table 1. Patients should be centrally placed in the scanner to ensure that the entire pulmonary parenchyma is covered by the smaller field-of-view of the second tube detector array (the field-of-view of the second tube detector array is 260 mm or 330mm) when dual source CT was used.

3.2 Contrast Medium injection protocols

High-concentration iodine-based contrast material is recommended for DECT scans to improve the differentiation of iodine by the dual-energy post-processing algorithm. As mentioned above in the section of scanning protocols, thoracic DECT scans should be acquired in the caudo-cranial direction so that the chaser bolus is being injected by the time

	Siemens Definition	Siemens Definition Flash
Scan mode	Spiral dual energy	Spiral dual energy
Scan area	Diaphragm to lung apex	Diaphragm to lung apex
Scan direction	Caudo-cranial/cranio-caudal	Caudo-cranial/cranio-caudal
Scan time(s)(for 300 mm length)	10	9
Tube voltage A/B (kVp)	140/80	100/140Sn (tin filter)
Tube current A/B (quality ref. mAs)	51/213	89/76
Dose modulation	CARE Dose 4D	CARE Dose 4D
CTDIvol (mGy)	6	7.3
Rotation time (s)	0.33	0.28
Pitch	0.7	0.55
Slice collimation (mm)	1.2	0.6
Acquisition (mm)	14x1.2	128x0.6
DE composition factor	0.3	0.6
Reconstruction kernel	D30f	D30f

Table 1. Scan protocols recommended for a dual-energy lung perfusion scan on the currently available dual-source CT systems (Siemens Healthcare)

the scan reached the upper chest to avoid streak artifacts due to highly concentrated contrast material in the subclavian vein or superior vena cava. In order to acquire both pulmonary arteries and lung perfusion in an optimal scan, the scan delay should be a little longer (e.g.4-7s) to allow the contrast material to pass into the lung parenchyma. Bolus tracking should be used for timing with the region of interest placed in the pulmonary artery trunk. There was no significant difference in pulmonary artery enhancement between test bolus and automatic bolus tracking in previously performed studies [Geyer LL, 2011]. Therefore, automatic bolus tracking is recommended because it is operator friendly and independent. The patient should be instructed to hold his breath at mild inspiration to avoid excessive influx of non-enhanced blood from the inferior vena cava. Contrast injection protocol of dual source dual-energy CT pulmonary angiography is seen in Table 2.

	Iodine concentration 300mg I ml ⁻¹	Iodine concentration 370mg I ml ⁻¹	Iodine concentration 400mg I ml ⁻¹
Contrast media volume (ml kg ⁻¹)	1.5	1.2	1.1
Contrast media flow rate (ml s ⁻¹)	4	4	4
Bolus timing	Bolus tracking	Bolus tracking	Bolus tracking
Bolus tracking threshold(HU)	100	100	100
ROI position	Pulmonary trunk	Pulmonary trunk	Pulmonary trunk
Scan delay(s)	6	6	7
Saline flush volume(ml)	40	40	60
Saline injection rate(ml s ⁻¹)	4	4	4
Needle size(G)	18	18	18
Injection site	Antecubital vein	Antecubital vein	Antecubital vein

Table 2. Contrast injection protocol of dual-energy pulmonary CT angiography

4. Image post-processing and image interpretation

4.1 Image post-processing

From the raw spiral projection data of both tubes, images were automatically reconstructed to three separate image sets: 80 kVp, 140 kVp and average weighted virtual 120 kVp images with 80:140 kVp linear weighting of 0.3 (i.e. 30% image information from the 80 kVp image and 70% information from the 140 kVp image). For each image set, the slice thickness was 0.75 mm and interval was 0.50 mm. The only currently commercially available software (syngo DE Lung PBV by Siemens HealthCare) for DECT lung perfusion image analysis is part of the dual energy post-processing software package available for the Siemens syngo MultiModality Workplace. For the calculation of iodine distribution in the lung parenchyma, the application class is designed for iodine extraction, and the material parameters for iodine extraction are as follows: -1,000 HU for air at 80 kVp, -1,000 Hounsfield unit (HU) for air at 140 kVp, 60 HU for soft tissue at 80 kVp, 54 HU for soft tissue at 140 kVp, 2 for relative contrast enhancement, -960 HU for minimum value, -200~-300 HU for maximum value, and 4 for range (Figure 1A). The lung parenchyma is color coded using gray scale 16-bit or hot metal 16-bit color coding (default setting) with different optional color scales available. The software enables a multiplanar view of the lung parenchyma image. The software also enables users to set a mixing ratio between a non color-coded virtual 120 kV dataset and color-coded lung parenchyma. This mixing ratio can be fluently set between 0% showing a anatomy image and 100% showing a blood flow image (BFI) images where only the color-coded, segmented lung parenchyma is displayed. Windowing functionality for the original and color-coded dataset, basic measurement tools, and a few dual-energy-specific measurements are also available. The fused images are obtained by mixing the anatomy image and BFI images with different ratios. The fused images are used for visualization of CT pulmonary angiography and the lung perfusion.

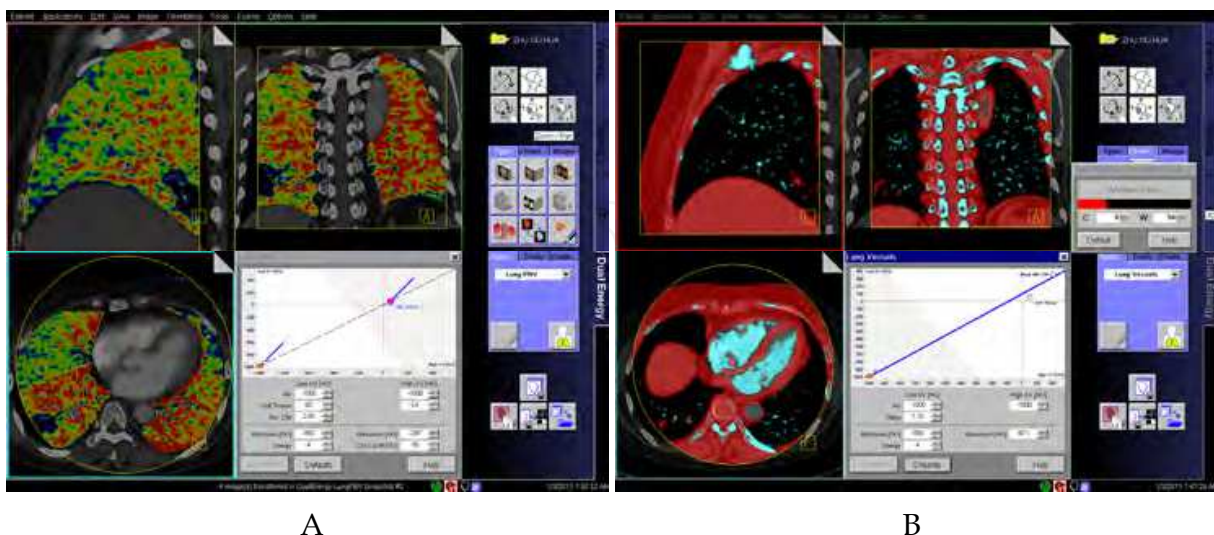


Fig. 1. Parameter settings of the postprocessing software for dual energy CT pulmonary angiography

A) Parameter settings of Lung Pulmonary Blood Volume (PBV) software; B) Parameter settings of Lung Vessels software

The Lung Vessels application was developed to discriminate non-enhancing subsegmental pulmonary arteries from enhancing ones by using dual energy iodine extraction data. This technique had a high negative predictive value being important for exclusion of segmental PE. In the Lung Vessels application, results are displayed as color-coded multi planar reformatted data and a 3D volume rendered dataset, where vessels with high iodine content are color-coded blue and soft tissue or vessels with low or no iodine content due to PE are color-coded red. The material parameters for iodine extraction of Lung Vessels are as follows: -1,000 HU for air at 80 kVp, -1,000 Hounsfield unit (HU) for air at 140 kVp, 60 HU for soft tissue at 80 kVp, 54 HU for soft tissue at 140 kVp, 1.1 for relative contrast enhancement, -500 HU for minimum value, 3071 HU for maximum value, and 4 for range (Figure 1B).

4.2 BFI image interpretation

It is very important to recognize the normal findings or artifacts at DECT lung perfusion. Normal pulmonary BFI images were defined as showing homogeneous perfusion in the normal range (color-coded yellow-green or blue) with dependent symmetric lung iodine distribution (Figure 2). Dependent lung perfusion at DECT refers to relatively low contrast enhancement in the ventral regions (color coded yellow-green) and relatively higher enhancement in the dorsal regions (color coded blue -black) with the patient in the supine position (Figure 3).

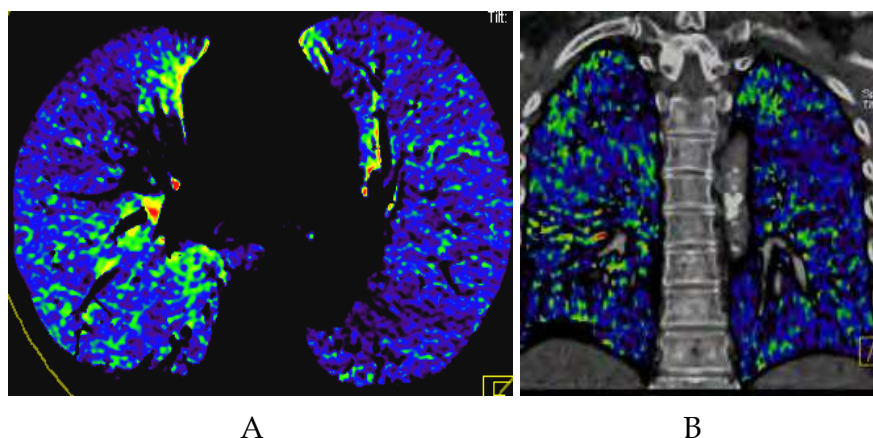


Fig. 2. Normal pulmonary blood flow imaging

A) Axial BFI image and B) coronal fused image show homogeneous blood flow distribution in both lungs

In the analysis of BFI images, sources of pitfall should be kept in mind to avoid misdiagnoses. When interpreting BFI images, these pitfalls can relate to artifacts from contrast material, diaphragmatic or cardiac motion, pulmonary pathology and the occlusive degree of pulmonary arteries.

Streak and beam-hardening effects resulting from high-concentration contrast agent in the thoracic veins and right cardiac chambers can commonly cause heterogeneous artifacts in BFI images (Figure 4); these artifacts must be considered when an unexpected contrast enhancement defect is noted adjacent to an area of high contrast enhancement. In this setting, the perfusion defect may appear band-like and be mostly in both upper lobes. Optimization of contrast medium injection parameters, including the use of a saline chaser, can reduce the beam-hardening artifact, improve the image quality of DECT and increase

diagnostic confidence. Nance JW Jr et al [Nance JW Jr,2011] reported that iomeprol 400 at 4 mL/s (an IDR of 1.6 g I/s) resulted in superior quality CTPA and perfusion map images compared with the protocols using a lower concentration or delivery rate.

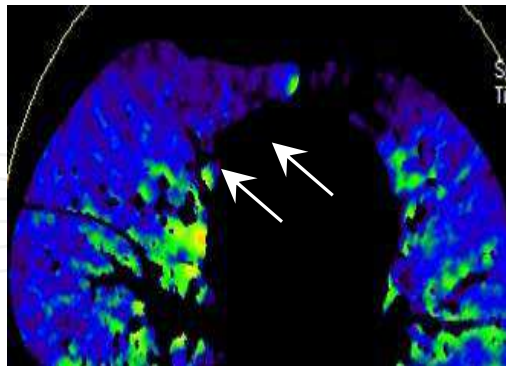


Fig. 3. Gravity-dependent lung perfusion states

A normal pulmonary BFI image obtained in one patient in the supine position shows relatively low pulmonary contrast enhancement anteriorly (arrows) and relatively high contrast enhancement in more dependent lung portions

Diaphragmatic or cardiac motion can cause apparent lower areas of lung contrast enhancement in the lung parenchyma adjacent to the diaphragm or cardiac chambers (Figure 5). In this setting, the perfusion defect is crescent-shaped; blurring or double lines adjacent to the diaphragm or heart border can be seen on images obtained with lung windows or mediastinal windows. Patients should hold their breath while scanning to reduce the diaphragm motion artifacts. A potential method to improve image quality in the vicinity of the cardiac chambers might be to synchronize data acquisition with electrocardiographic tracing, a technological development currently exclusively available for myocardial “perfusion” analysis [Pontana F,2008]; however, such methodology could also potentially introduce stair-step or misregistration artifacts and requires further study. Normal physiological gravity dependent variation in pulmonary “perfusion” should also be recognized [Zhang LJ,2009(Eur Rdiol)/2009(Acta Radio)].

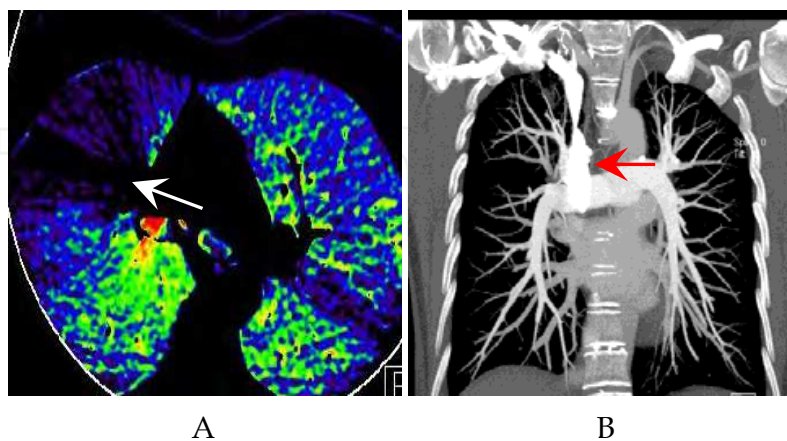


Fig. 4. Pseudo-high perfusion due to dense contrast material in the superior vena cava
A) An axial BFI image shows radiating pseudo-high perfusion and pseudo-iodine defect adjacent to the superior vena cava (white arrow) due to streak artifact from high concentration contrast material. B) Coronal maximum intensity projection image shows a higher opacity of superior vena cava (red arrow) than pulmonary artery

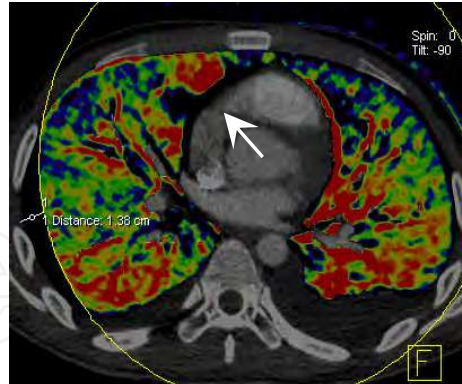


Fig. 5. Cardiac motion artifact

Crescent-shaped perfusion defect is seen in the lung parenchyma adjacent to the cardiac chambers (white arrow)

In addition, the anatomy CT images should be evaluated for pulmonary pathology, such as emphysema (Figure 6), tumors invading or compressing the pulmonary arteries (Figure 7) and pulmonary consolidation (Figure 8), all of which will result in contrast enhancement defects in BFI images. The occlusive degree of pulmonary arteries will affect perfusion defects at BFI and result in the false-negatives (Figure 9). But, misdiagnosis resulting from these factors is rare when BFI images are interpreted in conjunction with CTPA, which can reliably detect the lobar and segmental emboli. Nevertheless, small peripheral pulmonary emboli causing minimal contrast enhancement defect alterations can be overlooked even when state-of-the-art MDCT scanners are employed. Also, the considerable reduction in the pulmonary capillary bed often seen in the elderly or patients with emphysema can cause diffuse decreased pulmonary “perfusion” [Boroto K, 2008].

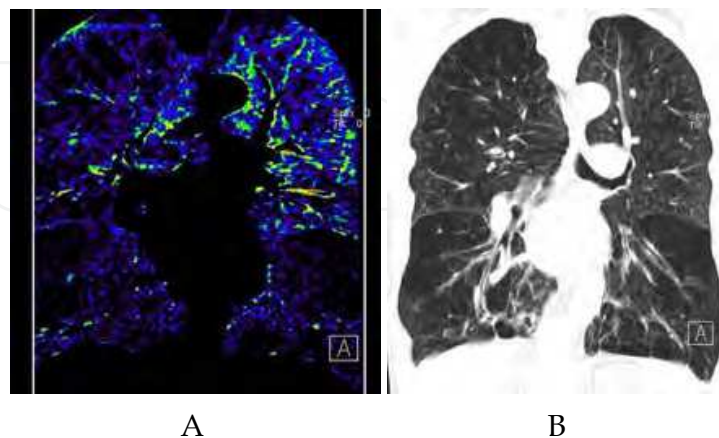


Fig. 6. Contrast defect in the BFI image caused by emphysema

A) A coronal BFI image shows heterogeneous contrast enhancement in both lungs caused by the emphysema that is readily seen at coronal reformatted multiplanar reformation viewed with lung windows (B)

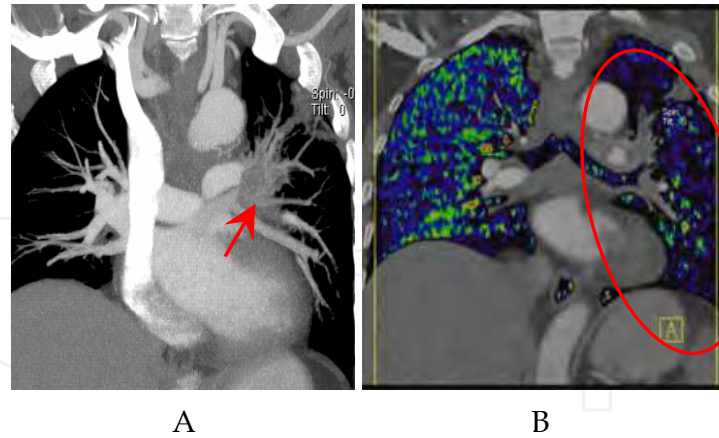


Fig. 7. Contrast defect in the pulmonary blood volume image caused by lung carcinoma
 A) A coronal MIP image shows a left lung hilar carcinoma invading the left pulmonary lobar arteries (red arrow), resulting in diffuse decreased contrast enhancement of the left lung (red circle) at the corresponding coronal BFI image fused with the CT angiogram (B)

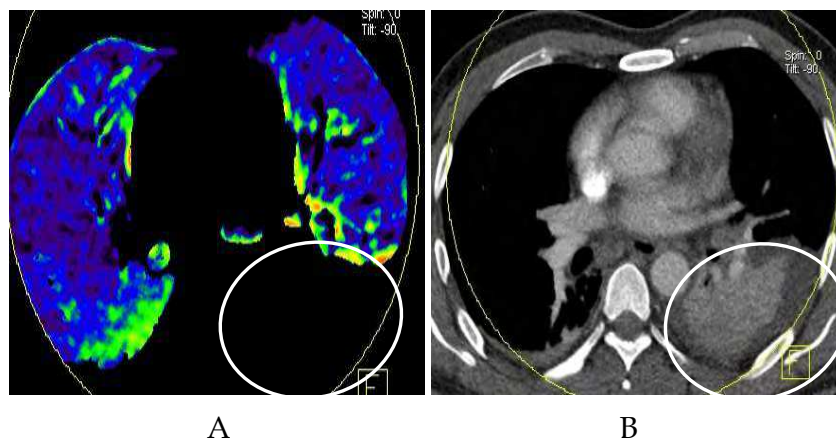


Fig. 8. Contrast enhancement defect in the pulmonary blood volume image caused by lung consolidation
 A) Axial BFI image shows a contrast enhancement defect in the left lower lobe (white circle);
 B) The corresponding axial CT image clearly shows pulmonary consolidation in the corresponding left lower lung lobe (white circle)

5. Clinical applications

5.1 Acute PE detection

Perfusion defects that are consistent with acute PE include those that are peripherally located, wedge-shaped, and in a segmental or lobar distribution (Figure 10). All other perfusion defects, such as patchy or band-like defects without segmental distribution, or complete loss of color-coding (indicating lack of air-containing voxels due to consolidation), were considered to be inconsistent with PE. For the Lung Vessels application, color-coded red PAs was regarded as positive for PE (Figure 11), while color-coded red soft tissue around PAs was discarded.

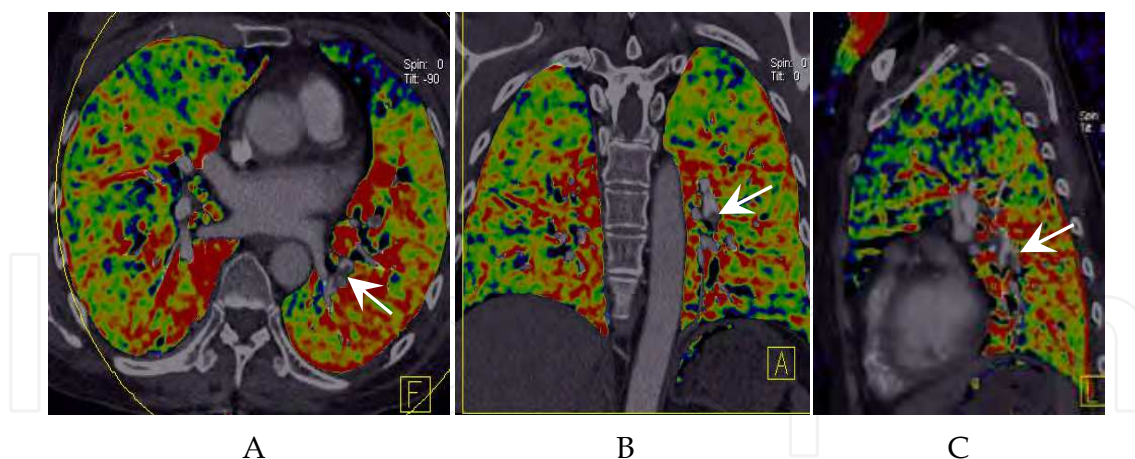


Fig. 9. Negative BFI image in one patient with left lower pulmonary artery embolus
A) axial, B) coronal, and C) sagittal fused images show normal findings with non-occlusive PE(white arrow) and result in the false-negatives

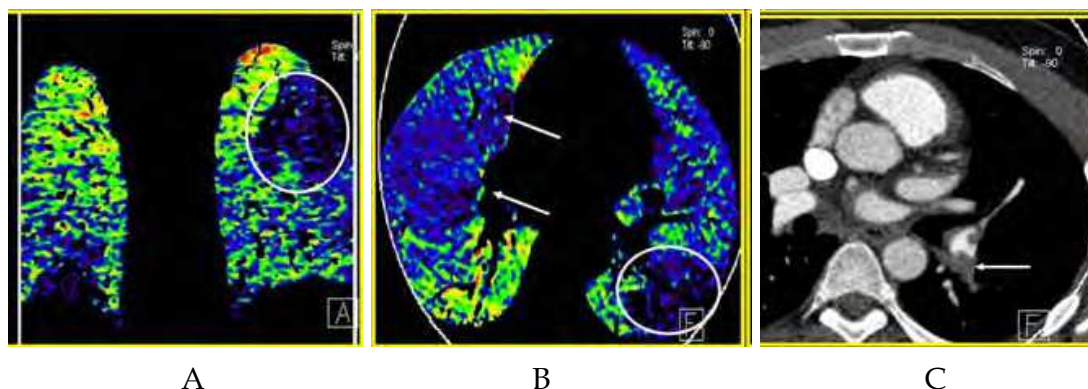


Fig. 10. Acute PE in a 24-year-old man
A) Coronal and B) Axial BFI images show a wedge-shaped perfusion defect in the left lung lower lobe dorsal segment (white circle). Pseudo-high contrast enhancement is seen in the anterior portion of the right middle lung anterior to the normal pulmonary contrast enhancement seen in the right middle lobe more posteriorly (arrows). C) Axial contrast-enhanced CT image shows a corresponding occlusive filling defect representing pulmonary emboli in the left lower lobe segmental pulmonary arteries (arrow), and non-occlusive emboli elsewhere

Several studies have examined DECT for the detection of PE. Fink et al [Fink C, 2008] reported that both sensitivity and specificity of DECT for the assessment of PE were 100% on a per patient basis. On a per segment basis, the sensitivity and specificity ranged from 60%–66.7% and from 99.5%–99.8%; CTPA was used in this study as the standard of reference in 24 patients with suspected PE, 4 of whom actually had PE. With scintigraphy as the standard of reference, Thieme et al [Thieme SF, 2008] reported 75% sensitivity and 80% specificity on a per patient basis and 83% sensitivity and 99% specificity on a per segment basis in a small group of patients with DECT. A group of 117 patients was examined by Pontana et al [Pontana F, 2008] to investigate the accuracy of DECT in the depiction of perfusion defects in patients with acute PE, concluding that simultaneous information on the presence of endoluminal thrombus and lung perfusion impairment can be obtained with

DECT. In an experimental study by Zhang et al [Zhang LJ ,2009], conventional CTPA identified pulmonary emboli in only 12 and the absence of emboli in 18 pulmonary lobes, corresponding to a sensitivity and specificity of 67% and 100%. In contrast, DECT and BFI each correctly identified pulmonary emboli in 16 of 18 pulmonary lobes and reported the absence of emboli in 11 of 12 lobes, corresponding to sensitivity and specificity of 89% and 92% for detecting pulmonary emboli. Thus, pulmonary CTA and DECT lung perfusion have complimentary roles in the diagnosis of PE and DECT lung perfusion images increase the sensitivity for detection of PE (Figure 12), particular for tiny peripheral emboli [Lu GM ,2010]. It can be presumed that a simultaneous detection of a clot in a pulmonary artery in the pulmonary CTA and of a corresponding perfusion defect in DECT lung perfusion indicate an occlusive PE.

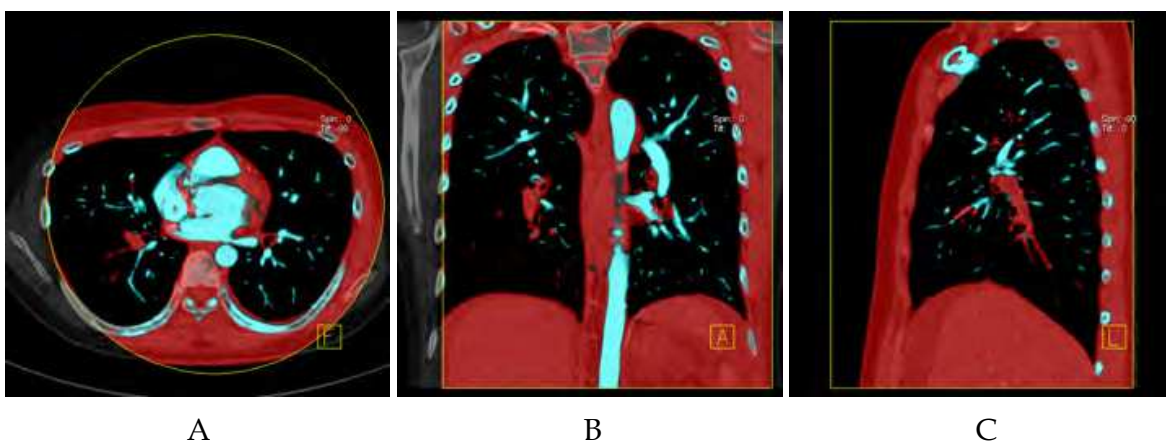


Fig. 11. Acute pulmonary embolism in one 17-year-old man
A) axial, B) coronal, and C) right sagittal lung vessel images show the pulmonary emboli in the right lower pulmonary artery color coded as red

Furthermore, pulmonary CTA and DECT lung perfusion could assist in the detection of pulmonary emboli that are not evident by conventional MDCT pulmonary angiography. Thieme et al [Thieme SF ,2008] found that corresponding perfusion defects were observed in DECT and scintigraphy in two patients in whom there was no evidence of intravascular clots in angiographic CT images. They proposed that the observed pulmonary perfusion defects probably corresponded to segments of prior embolism with re-perfused, segmental vessels and residual peripheral thrombosed vessels that were too small to visualize in CTPA. The same assumption was also made in the study by Pontana et al [Pontana F, 2008], in which four subsegmental perfusion defects were depicted by BFI images, whereas endoluminal thrombi were not visualised in the corresponding arteries by CTPA. Zhang et al [Lu GM ,2010] also found a similar so-called false-positive DECT result in one patient with chronic PE in the pulmonary images of BFI. In another patient undergoing anticoagulant therapy, the conventional CTPA performed initially did not visualize abnormal findings. However, the magnified view of the targeted pulmonary arteries corresponding to contrast enhancement defect in the BFI images showed a subtle subsegmental filling defect. These findings indicate that CTPA might not be an adequate gold standard to detect all PE, especially for the small peripheral emboli or chronic PE. However, this does not mean to deny the mainstay role of MDCT in the evaluation of pulmonary emboli. The detection of small emboli is of clinical importance because even

small emboli require treatment to prevent chronic PE and pulmonary artery hypertension in several clinical scenarios in patients with a small embolus and inadequate cardiopulmonary reserve; in patients who have a small embolus and coexisting acute deep venous thrombosis; and in patients with recurrent small emboli possibly owing to thrombophilia [Remy-Jardin M, 2007]. Certainly, the significance of small emboli needs further study.

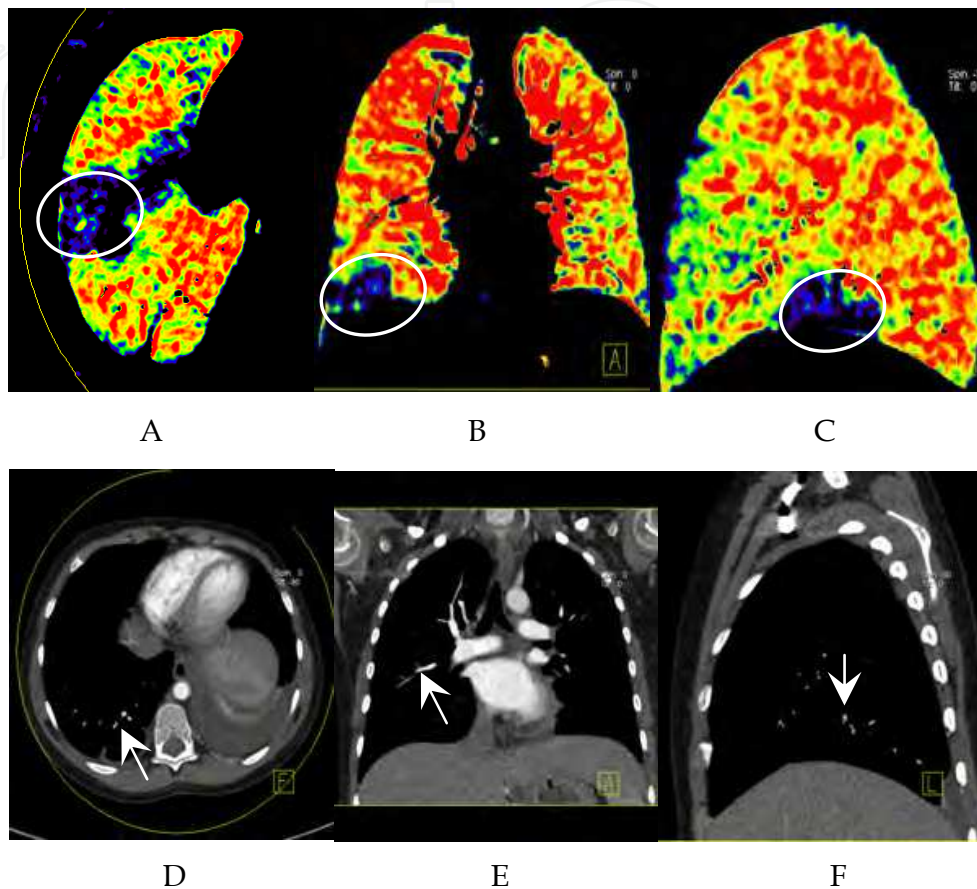


Fig. 12. Tiny peripheral emboli in right lower pulmonary artery

A) Axial, B) coronal, and C) left sagittal BFI images show a wedge-shaped perfusion defect in the right lung lower lobe dorsal segment (white circle); D) Axial, E) coronal, F) left sagittal contrast-enhanced CT image shows no filling defect in the corresponding right lower pulmonary artery (white arrow)

5.2 Evaluation of PE severity

In patients with acute PE, rapid risk assessment is critical because high-risk patients may benefit from life-saving thrombolytic therapy or invasive therapies, including catheter-guided thrombosuction or thrombectomy [Dogan H, 2007]. Right heart strain (RHS) has been shown to be independently predictive of 30-day mortality. In addition to use as a CT marker of RHS, the ratio between the size of the right ventricle (RV) and left ventricle (LV) has demonstrated a significant positive correlation with severity of PE and mortality [Ghaye B, 2006]. Chae et al. [Chae EJ, 2010] and Zhang et al [Zhang LJ, 2009(Acta Radio)] reported good correlation between RV/LV diameter ratio with a novel self-defined dual energy perfusion score or the number of pulmonary segments with perfusion defects, respectively.

Recently, Bauer RW et al [Bauer RW, 2011] reported patients with RHS had significantly higher perfusion defect (PD) size than patients without RHS and confirm that PD size can be seen as marker for RHS. Bauer RW et al [Bauer RW, 2011] also reported that looking at the incidence of readmission and death due to PE demonstrated these major hard endpoints only in patients with a relative PD size of >5% of the total lung volume, whereas no such event was recorded for patients with <5% RelPD (relatively to the total lung volume, RelPD). Median survival time, however, was significantly lower for patients with >5% RelPD at an increased relative hazard ratio for death compared to patients with <5% RelPD or the control group without PE. Thus, PD size might even be an additional instrument for prognostic evaluation in PE itself.

6. Chronic PE

DECT pulmonary angiography can also allow for the depiction of perfusion defects in patients with chronic PE or patients with chronic thromboembolic pulmonary hypertension (CTEPH). A typical imaging characteristic of chronic PE can be mosaic patterns of lung attenuation, that is, areas of ground-glass attenuation mixed with areas of normal lung attenuation, suggesting a redistribution of blood flow.

These perfusion defects in BFI beyond chronic clots, similar to what is achievable for acute PE, and these changes closely mirror the mosaic attenuation pattern which is very suggestive of blood flow redistribution in CTEPH. Mosaic attenuation can sometimes be subtle, and BFI appears to accentuate regional differences in parenchymal attenuation, which become very conspicuous when displayed as a color map. In CTEPH, DECT can identify matched defects (i.e., occluded pulmonary arteries to lobe and negligible residual blood flow), mismatched defects (i.e., occluded lobar artery and demonstrable residual blood flow), and normal lung regions (i.e., unobstructed pulmonary arteries with demonstrable normal or increased flow). Perhaps of most interest are areas of mismatch where there is blood supply maintained beyond the occluded pulmonary arteries [2].

7. Radiation dose

There are concerns about radiation dose of DECT pulmonary angiography. For a DECT pulmonary angiography variable dose length product (DLP) have been reported (range, 143-302 mGy*cm) [Schenzle JC, 2010; Zhang LJ, 2009; Thieme SF, 2010] depending on the acquisition parameters, especially on the mAs settings. This value is lower than the published DLP of chest CT for PE (882 mGy*cm) and similar to the previously published DLP of routine chest CT (411 mGy * cm). Pontana et al [Pontana F , 2008] reported that the mean DLP of DECT pulmonary angiography for PE is 280 mGy *cm, corresponding to an average effective patient dose of about 5 mSv. Kang et al [Kang MJ, 2010] reported that the mean DLP of DECT with the PE protocol was 376 mGy*cm. All reported values for pulmonary DECT imaging are substantially lower than the reference value of 650 mGy*cm from the European guidelines on quality criteria for CT. Thus, even if the dose of DECT of the thorax can be a little bit higher than the dose values reported for a standard, single-source, single-energy thoracic CT, the above-mentioned benefits of DECT of the lung in patients with suspected PE seem to justify the moderate increase in the overall radiation dose. It is the only technique allowing for a direct comparison of CT angiograms acquired at

different energies in the same patient, at the same time point after the injection of the contrast medium, and within strictly similar hemodynamic conditions.

8. Conclusion

DECT can provide both anatomical and iodine mapping information of the whole lungs in a single contrast-enhanced CT scan. After recognition of some artifacts in DECT pulmonary angiography, this technology has the capacity to improve the detection and severity evaluation of acute and chronic PE through comprehensive analysis of BFI and CT pulmonary angiography obtained during a single contrast-enhanced chest CT scan in a dual-energy mode. DECT pulmonary angiography can be used as a one-stop-shop technique for the evaluation of PE.

9. Acknowledgement

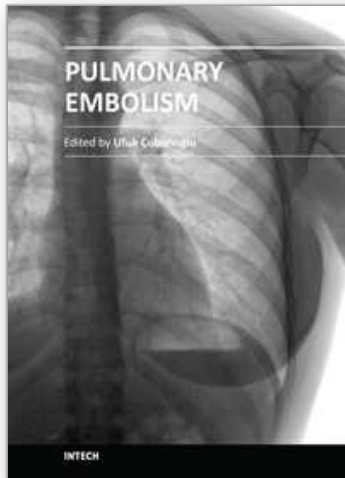
Long Jiang Zhang received the grant from the Peak of six major talents of Jiangsu Province Grant (No. WSW-122 for L.J. Z.).

Guang Ming Lu received the grant from the Natural Science Foundation of Jiangsu Province of China (No. BK2009316 for G.M.L.).

10. References

- Boroto K, et al. (2008). Thoracic applications of dual-source CT technology. *Eur J Radiol* 68(3):375-84.
- Bauer RW, et al. (2011). Dual energy CT pulmonary blood volume assessment in acute pulmonary embolism - correlation with D-dimer level, right heart strain and clinical outcome. *Eur Radiol* 21(9): 1914-1921.
- Chae EJ, et al. (2010). Dual-energy CT for assessment of the severity of acute pulmonary embolism: pulmonary perfusion defect score compared with CT angiographic obstruction score and right ventricular/left ventricular diameter ratio. *Am J Roentgenol* 194(3):604-610.
- Dogan H, et al. (2007). Right ventricular function in patients with acute pulmonary embolism: analysis with electrocardiography-synchronized multi-detector row CT. *Radiology* 242(1):78-84.
- Fink C, et al. (2008) Dual-energy CT angiography of the lung in patients with suspected pulmonary embolism: Initial results. *Rofo* 180(10):879-883.
- Geyer LL, et al. (2011). Imaging of acute pulmonary embolism using a dual energy CT system with rapid kVp switching: Initial results. *Eur J Radiol* Mar 18. [Epub ahead of print]
- Ghaye B, et al. (2006). Severe pulmonary embolism: pulmonary artery clot load scores and cardiovascular parameters as predictors of mortality. *Radiology* ;239(3):884-91.
- Kang MJ, et al. (2010) Dual-energy CT: clinical applications in various pulmonary diseases. *Radiography* 30(3):685-698.
- Lu GM, et al. (2010). Dual-energy computed tomography in pulmonary embolism. *Brit J Radiol* 83(992):707-718.
- Laack TA & Goyal DG. (2004). Pulmonary embolism: an unsuspected killer. *Emerg Med Clin North Am* 22:961-983.

- Nance JW Jr, et al. (2011). Optimization of contrast material delivery for dual-energy computed tomography pulmonary angiography in patients with suspected pulmonary embolism. *Invest Radiol* May 13. [Epub ahead of print].
- Pontana F, et al. (2008). Lung perfusion with dual-energy multidetector-row CT (MDCT): feasibility for the evaluation of acute pulmonary embolism in 117 consecutive patients. *Acad Radiol* 15(12):1494–1504.
- Patel S, et al. (2003). Pulmonary embolism: optimization of small pulmonary artery visualization at multidetector row CT. *Radiology* 227(2):455–460.
- Remy-Jardin M, et al. (2007). Management of suspected acute pulmonary embolism in the era of CT angiography: a statement from the Fleischner Society. *Radiology* 245(2):315–29.
- Schoepf UJ, et al. (2000). Pulmonary embolism: comprehensive diagnosis by using electron-beam CT for detection of emboli and assessment of pulmonary blood flow. *Radiology* 217(3):693–700.
- Schenzle JC, et al. (2010). Dual energy CT of the chest—How about the dose? *Invest Radiol* 45(6): 64-71.
- Thieme SF, et al. (2010). Dual-energy lung perfusion computed tomography: a novel pulmonary functional imaging method. *Semin Ultrasound CT MR* 31(4):301-308.
- Thieme SF, et al. (2008). Dual energy CT for the assessment of lung perfusion—correlation to scintigraphy. *Eur J Radiol* 68(3):369–74.
- Tapson VF. (2008). Acute pulmonary embolism. *N Engl J Med* 358(10):1037–1052.
- Thieme SF, et al. (2009). Dual-energy CT for the assessment of contrast material distribution in the pulmonary parenchyma. *AJR Am J Roentgenol* ;193(1):144-149.
- Wildberger JE, et al. (2001). Multi-slice CT for visualization of pulmonary embolism using perfusion weighted color maps. *Rofo* 173(4):289–294.
- Wildberger JE, et al. (2005). Multislice computed tomography perfusion imaging for visualization of acute pulmonary embolism: animal experience. *Eur Radiol* 15(7):1378–1386
- Zhang LJ, et al. (2009). Detection of pulmonary embolism by dual energy CT: correlation with perfusion scintigraphy and histopathological findings in rabbits. *Eur Radiol* 19(12): 2844–2854.
- Zhang LJ, et al. (2009). Detection of pulmonary embolism using dual-energy computed tomography and correlation with cardiovascular measurements: a preliminary study. *Acta Radiol* 50(8):892–901
- Zhang LJ, et al. (2009). Detection of pulmonary embolism by dual energy CT: an experimental study in rabbits. *Radiology* 252(1):61–70.



Pulmonary Embolism

Edited by Dr. Ufuk Çobanoğlu

ISBN 978-953-51-0233-5

Hard cover, 236 pages

Publisher InTech

Published online 14, March, 2012

Published in print edition March, 2012

Pulmonary embolism is a serious, potentially life-threatening cardiopulmonary disease that occurs due to partial or total obstruction of the pulmonary arterial bed. Recently, new improvement occurred in the diagnosis and treatment of the disease. The aim of this disease is to re-review pulmonary embolism in the light of new developments. In this book, in addition to risk factors causing pulmonary embolus, a guide for systematic approaches to lead the risk stratification for decision making is also presented. In order to provide a maximum length of active life and continuation of functional abilities as the aim of new interventional gerontology, the risk factors causing pulmonary embolus in elderly individuals are evaluated, and the approach to prevention and treatment are defined. The risk of the development of deep vein thrombosis and pulmonary embolism, combined with obesity due to immobility, the disease of this era, irregular and excessive eating, and treatment management are highlighted. Non-thrombotic pulmonary emboli are also covered and an attempt is made to constitute an awareness of this picture that can change the treatment and prognosis of the disease to a considerable extent. In addition to the pathophysiological definition of pulmonary embolus, the priority goal of quick and definitive diagnosis is emphasized, and diagnostic strategies are discussed in the book. A numerical analysis of the vena cava filters, which is a current approach to prevent pulmonary emboli recurrences, is presented in the last chapter.

How to reference

In order to correctly reference this scholarly work, feel free to copy and paste the following:

Yan'E Zhao, Long Jiang Zhang, Guang Ming Lu, Kevin P. Gibbs and U. Joseph Schoepf (2012). Dual Source, Dual Energy Computed Tomography in Pulmonary Embolism, Pulmonary Embolism, Dr. Ufuk Çobanoğlu (Ed.), ISBN: 978-953-51-0233-5, InTech, Available from: <http://www.intechopen.com/books/pulmonary-embolism/dual-source-dual-energy-computed-tomography-in-pulmonary-embolism>

INTECH
open science | open minds

InTech Europe

University Campus STeP Ri
Slavka Krautzeka 83/A
51000 Rijeka, Croatia
Phone: +385 (51) 770 447
Fax: +385 (51) 686 166

InTech China

Unit 405, Office Block, Hotel Equatorial Shanghai
No.65, Yan An Road (West), Shanghai, 200040, China
中国上海市延安西路65号上海国际贵都大饭店办公楼405单元
Phone: +86-21-62489820
Fax: +86-21-62489821

www.intechopen.com

www.intechopen.com

IntechOpen

IntechOpen

© 2012 The Author(s). Licensee IntechOpen. This is an open access article distributed under the terms of the [Creative Commons Attribution 3.0 License](#), which permits unrestricted use, distribution, and reproduction in any medium, provided the original work is properly cited.

IntechOpen

IntechOpen